Steel and Composite Structures, Vol. 10, No. 3 (2010) 281-295 281
DOI: http://dx.doi.org/10.12989/scs.2010.10.3.281

Experimental and numerical analysis of composite beams strengthened by CFRP laminates in hogging moment region

A.M. El-Shihy, H.M. Fawzy, S.A. Mustafa* and A.A. El-Zohairy

Department of Structural Engineering, Faculty of Engineering, Zagazig University, P.O. Box 44519 Zagazig, Egypt

(Received December 14, 2009, Accepted June 07, 2010)

Abstract. An experimental and a non linear finite element investigation on the behavior of steel-concrete composite beams stiffened in hogging moment region with Carbon Fiber Reinforced Plastics (CFRP) sheets is presented in this paper. A total of five specimens were tested under two-point loads. Three of the composite beams included concrete slab while the other two beams had composite slabs. The stiffening was achieved by attaching CFRP sheets to the concrete surface at the position of negative bending moment. The suggested CFRP sheets arrangement enhanced the overall beam behavior and increased the composite beam capacity. Valuable parametric study was conducted using a three dimensional finite element model using ANSYS program. Both geometrical and material nonlinearity were included. The studied parameters included CFRP sheet arrangement, concrete strength and degree of shear connection.

Keywords: composite beams; CFRP; hogging moment; strengthening.

1. Introduction

Deterioration of structures is becoming a major concern to the civil engineering community. In certain cases structures are considered deficient if they are not capable of carrying applied loads. So there is an increasing need to strengthen and upgrade structures for several reasons such as expired design life, change in functionality, potential damage caused by mechanical actions and environmental effects, more stringent design requirements, original design and construction errors. Several methods for strengthening structures have been developed such steel plate bonding, steel patching and stitching techniques. These methods have several disadvantages associated with the transportation, corrosion of the plates, limited delivery lengths of plates and handling and installation of heavy plates, which necessitates the need for massive and expensive formwork to hold the plates in position during adhesive cure. Therefore, an alternative material was required for this structural strengthening method.

In recent years, the development of Fiber Reinforced Polymer (FRP) material, with a high-strength-to-weight ratio and excellent resistance to electrochemical corrosion Donnet and Bansal (1990), Gibson (1994), Kaw (1997), makes it particularly suited to structural applications. Field application of repair by epoxy-bonded FRP laminates is now recognized to be an effective and convenient method because of the good performance of FRP. In the literature, there are numerous articles reporting the behavior of

* Corresponding author, Ph., D., E-mail: suzanaa1@hotmail.com

virgin beams reinforced externally with FRP for the purpose of increasing the load-carrying capacity Teng and Smith (2002), Ashour *et al*. (2004),Buyukozturk *et al*. (2004), Gao *et al*. (2005). The reported studies have shown that externally bonded FRP can be effectively used to increase the strength and stiffness of reinforced concrete (RC) beams while maintaining an adequate level of deformability. Several organizations are developing extensive design guidelines for the use of carbon fiber reinforced polymer (CFRP), indicating that the process of standardization is underway. In contrast to the case for member strengthening, several experimental studies have focused on the use of CFRP sheet for the repair of load-damaged RC beams Sen *et al*. (1995), Mertz and Gillespie (1996), Wipf *et al*. (2007), Li *et al*. (2006). This paper presents an experimental and numerical analyses to predict the failure load of the steel-concrete composite beams with and without corrugated steel sheet strengthened in hogging moment region with Carbon Fiber Reinforced Plastics (CFRP) sheets. A parametric study was also presented to investigate the effect of CFRP sheet arrangement, concrete strength and degree of shear connection.

2. Experimental program

2.1 Test beam details

A total of five composite beams classified into two groups were tested under hogging moment. The first group was three specimens of composite beams without corrugated steel sheet; as shown in Fig. 1a. The second group included two specimens of composite beams with corrugated steel sheet; as shown in Fig. 1b. The slab used was 500 mm wide, 2,000 mm long and 100 mm thick. The steel I-beam used was S.I.B No. 200. All beams were tested in two-point loading over a simple span. Two beams were used as control specimens and the other three beams were strengthened in flexure using one and two layers of externally bonded CFRP laminates. The main flexural reinforcement consisted of three 10 mm bars with a sectional area of 235.7 mm^2; steel reinforcement ratio of 0.47%. The transverse reinforcement was ten 10 mm bars through the beam length. The tested specimens' data are summarized in Table 1.

2.2 Material properties

The yield strength of the steel I-beam was 360 N/mm^2 according to Product Data Sheet. The flange width

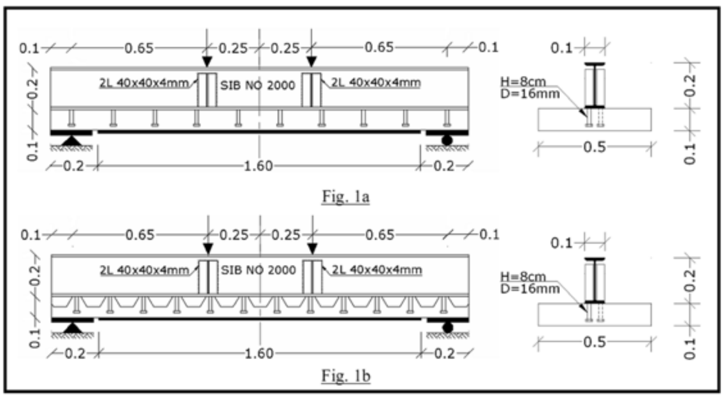

Fig. 1 Details of test beams (dimensions in m)

Table 1 Test specimen

	No.	Beam	No. of studs	Stud spacing	η^*	No. of CFRP strips
Group one	1	F1	10	200	1.0	-
	2	F2	10	200	1.0	3
	3	F3	10	200	1.0	6
Group two	1	C1	12	160	1.0	-
	2	C2	12	160	1.0	3

*η : degree of shear connection calculated according to BS 5950.

was suitable for the staggered arrangement of the stud shear connectors. A trapezoidal steel sheet was utilized in all tested specimens with corrugated steel sheet. The cover width of this type of sheet is 870 mm and thickness was 0.8 mm. The diameter of headed stud shear connectors was 14 mm and the height was 90 mm. For beams with corrugated sheet, the studs were welded to the steel I-beam through the steel sheet. The yield stress of the stud was 360 N/mm^2 and ultimate strength was 520 N/mm^2 according to Product Data Sheet. A tension test was performed on three pieces of the reinforcement bars, each of length 500 mm. The average yield stress was 360 N/mm^2, while the average ultimate tensile strength was 560 N/mm^2.

Concrete was designed with average grade of compressive strength of 30 Mpa. Six concrete cubes of side length of 150 mm were made at the time of casting and were kept with the beams during curing process. The average 28-day concrete cube strength f_{cu} was 30 MPa. The CFRP material consisted of 100 mm wide, 2,000 mm long and 0.12 mm thick carbon laminates. The sheets were externally bonded to the tension face of the concrete slabs using a two-part epoxy of Sikadur-330 mixed at 4 : 1 ratio by weight and cured at room temperature. The tensile strength of fiber was 4100 N/mm^2, tensile E-modulus of fibers was 231,000 N/mm^2 and the strain at break of fibers was 1.7%. The fabric design thickness of each layer of the CFRP strips was 0.12 mm based on total carbon content and the density was 1.78 g/cm^3.

2.3 Instrumentation

For each specimen, the steel I-beam and the concrete slab was instrumented with one electrical resistance strain gauge at mid-span. In addition, each test beam with CFRP laminates was instrumented with one strain gauge at mid-span. A total of two linear voltage displacement transducers (LVDTs) were used to measure mid-span, and loading point's deflection. A data logger was connected with the digital controller of the testing machine, strain gauges attached to the beams and LVDTs, for collecting the real time loading, strains and deflection. The reading was scanned at a time interval of 3 sec.

2.4 Test set-up and loading procedure

A typical set-up of the beam used in the experimental program is shown in Fig. 2. The total beam length was 2.0 m resting on supports of 1.8 m span. Every beam was inverted up-side-down with the concrete slab facing down. The vertical load was applied on the steel flange as two-point load. This loading technique made it possible to make the concrete exposed to moment simulating the existence of concrete in hogging moment region at the middle support in continuous composite beam. The same technique was used before by Loh *et al*. (2004).

Before the commencement of each test, a small load was applied to each beam specimen to check the specimen set-up, instrumentation and the loading system. The beams were loaded in a 2,000 kN test

a) Composite beam without corrugated steel sheet b) Composite beam with corrugated steel sheet

Fig. 2 Test set-up

frame with a loading rate of 350 N/sec. The loads were applied by screw jack fixed to the strong frame throughout the test procedure. The two load points were offset 250 mm from the mid-span of the beam; as illustrated in Fig. 1. The load was progressively increased up to failure of the specimens when no further load could be sustained.

3. Experimental results

The results of the tested five composite beams strengthened with CFRP sheets in hogging moment region are discussed in this section. A summary of the beam results is presented in Table 2.

3.1 Composite beams without corrugated steel sheet

For strengthened beams of group one, there was an increase in the load-carrying capacity when CFRP external reinforcement was added. The tested beams exhibited to two failure modes. Yielding in the tension steel reinforcement followed by failure in the concrete slab was noticed in control beam (F1); as illustrated in Fig. 3. For the strengthened beams (F2 and F3), rupture in the CFRP sheets accompanied by diagonal cracking in the longitudinal shear zone in the vicinity of the support was noticed; as illustrated in Figs. 4 and 5, respectively.

Fig. 6 shows the relation between load and deflection at mid-span for beams of group one. The load carrying capacity of the strengthened beam is higher than that of the control beam by 15% for beam strengthened with one layer (F2) and by 21% for beam strengthened with two layers (F3). It is noted that, increasing the CFRP thickness has increased the stiffness of the beam. The deflections corresponding to the yielding load and ultimate load are defined as yielding deflection Δ_y and ultimate deflection Δ_u,

Table 2 Results from composite beam tests

	Beam	P_{max} (ton)	δ_{max} (mm)	Failure mode
Group one	F1	29.8	33.8	Concrete Failure
	F2	32.4	24.7	Rupture in FRP
	F3	34.4	23.6	Rupture in FRP
Group two	C1	26.9	26.8	Concrete separation
	C2	29.9	26.9	Rib shear failure

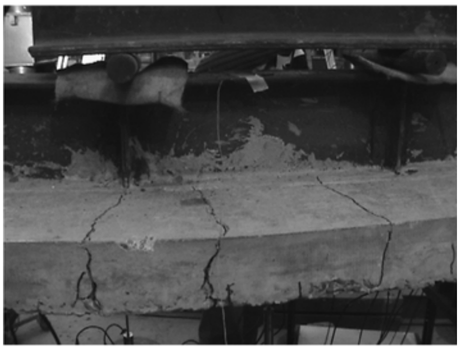

Fig. 3 Mode I failure: yielding in steel reinforcement and concrete failureg

Fig. 4 Mode II failure: rupture of CFRP

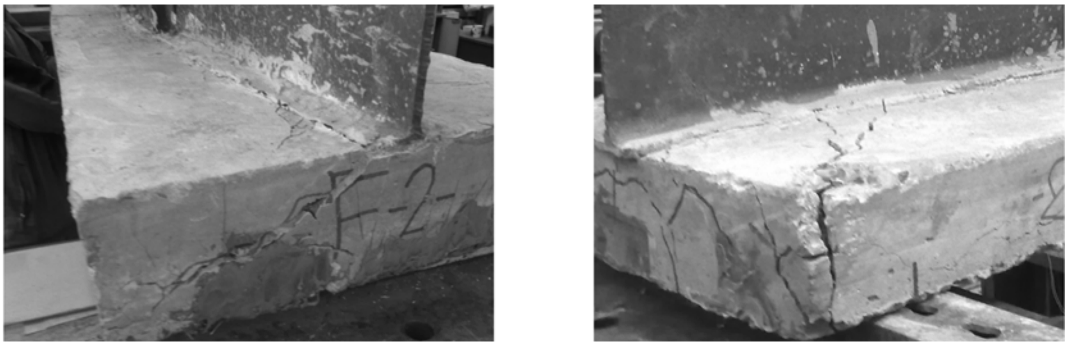

Fig. 5 Diagonal cracks in the vicinity of supports

respectively. The ductility of strengthened beam is defined as the ratio of ultimate deflection Δ_u to yielding deflection Δ_y. Compared to the control beam, all strengthened beams have less ultimate deflection. The ductility of strengthened beams has a range of 2.4 to 2.5 compared to 3.5 for the control beam. The low ductility of strengthened beams indicates that the addition of CFRP as reinforcement greatly reduces the deforming ability at the ultimate stage of loading.

Figs. 7, 8 and 9 show the load strain curves at mid-span of compression flange of the steel I-beam, tension surface of concrete slab and CFRP strips for tested beams of group one. A positive strain value

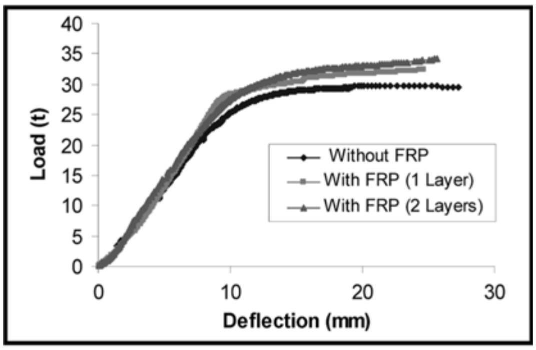

Fig. 6 Load vs. deflection

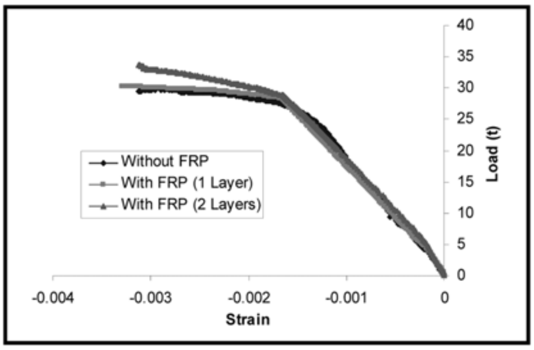

Fig. 7 Strain in steel I-beam flange

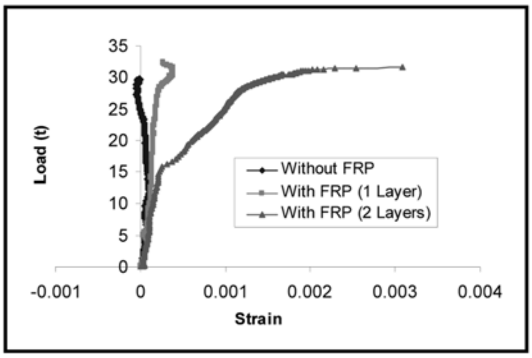

Fig. 8 Strain in concrete

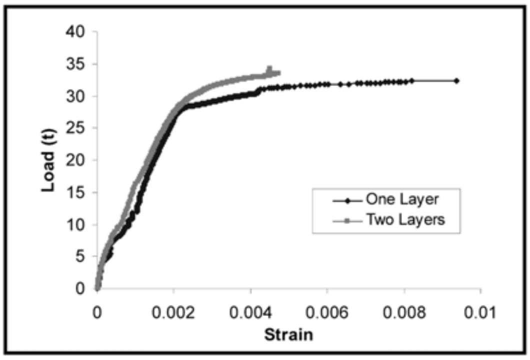

Fig. 9 Strain in CFRP strips

represents the tension strain in CFRP strips and concrete and a negative strain value indicates the compressive strain in the flange of the steel I-beam. It can be seen that each curve consists of three straight lines with different slopes. The first turning point indicates the cracking of concrete in tension zone. The second turning point refers to the yielding of tension steel. The yielding and maximum load can be found for each beam from its load-strain curve.

3.2 Composite beams with corrugated steel sheet

For strengthened beams of group two, there was a small increase in the load-carrying capacity when CFRP external reinforcement was added. The control beam (C1), failed by tensile cracks in the concrete surface of the composite slab followed by separation between the concrete slab and the corrugated steel sheet; as illustrated in Fig. 10. For the strengthened beam (C2), rib shear failure without any failure in the CFRP strips was noticed. The rib shear failure was accompanied with shear bond failure; as illustrated in Fig. 11. The presence of CFRP sheets delayed the cracks that used to happen in the concrete surface of the slab when exposed to bending.

Fig. 12 shows loads vs. deflection at mid-span for beams of group two. Deflection of the strengthened beam was reduced under the same load compared with the control beam by about 8.5%. The load carrying capacity of the strengthened beam was higher than that of the control beam by only 12%. Rib shear failure was observed in the strengthened specimen with no failure in the CFRP strips. It was therefore deduced that the width of the specimen was close to the limit beyond which rib-shear failure becomes critical. Figs. 13, 14 and 15 show the load strain curves at mid-span of compression flange of the steel I-beam, tension surface of concrete slab and CFRP strips for tested beams of group two.

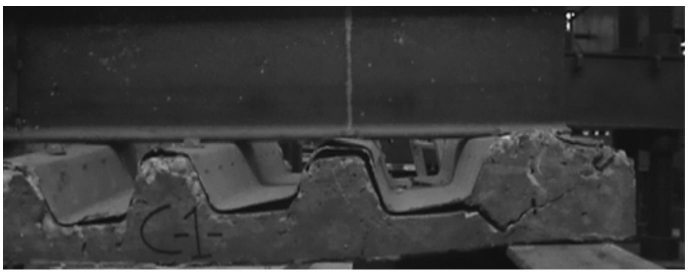

Fig. 10 Separation between the concrete and the steel corrugated sheet

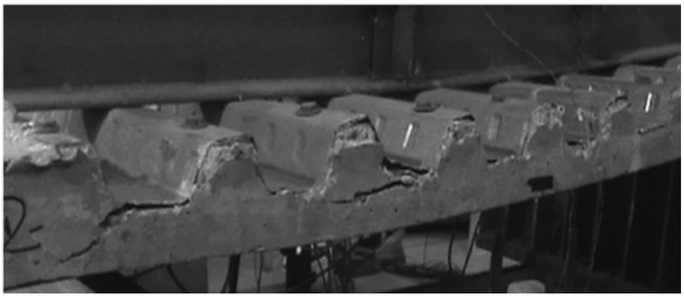

Fig. 11 Rib shear failure

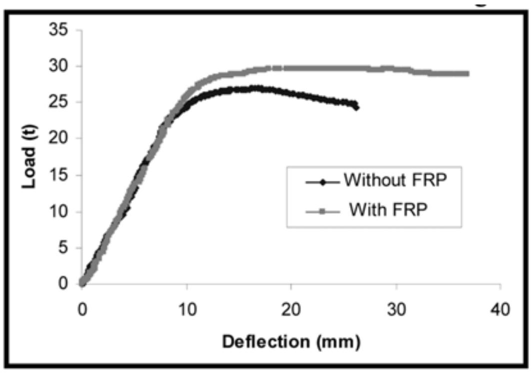

Fig. 12 Load vs. deflection

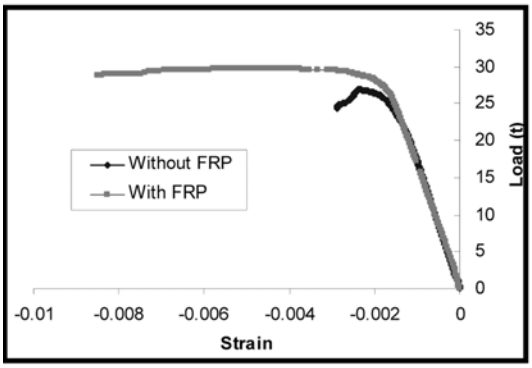

Fig. 13 Strain in steel I-beam flange

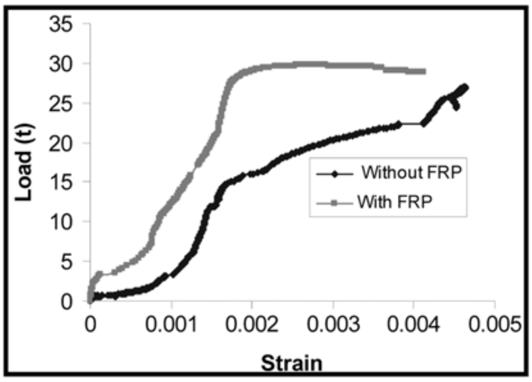

Fig. 14 Strain in concrete

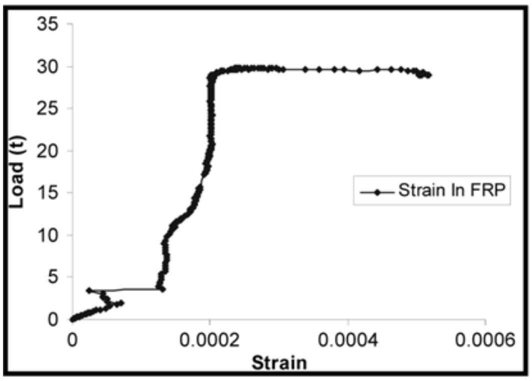

Fig. 15 Strain in CFRP strip

4. Numerical analysis

4.1 Finite element type and mesh

Along with the previous experimental investigation, a non-linear finite element study was performed using the software package **ANSYS** version 10. A three-dimensional finite element model has been developed to simulate the geometric and material non-linear behavior of the composite beams. The choice of the element type and mesh size were chosen carefully to obtain accurate results.

The element SOLID65 was used for the 3-D modeling of the concrete slab. It is capable of cracking in tension and crushing in compression. The element is defined by eight nodes having three degrees of freedom at each node. The element SHELL 43 was used to model the steel I-Beam web. It has six degrees of freedom at each node. The element has plasticity, creep, stress stiffening, large deflection, and large strain capabilities. The element SOLID45 was used for the 3-D modeling of steel I-beam flanges. This element is defined by eight nodes having three degrees of freedom at each node. The element has plasticity, hyperelasticity, stress stiffening, creep, large deflection, and large strain capabilities. The shear connectors were modeled using two different elements. The first element was a uniaxial element with tension-compression and bending capabilities and has three degrees of freedom at each node (BEAM23) which was directed to carry the axial load. This element has the ability to include or exclude shear deflection in its behavior. The second element was a unidirectional element with nonlinear generalized force-deflection capability and has three degrees of freedom at each node (COMBINE39) which was set to carry the shear that may happen between the steel I-beam and the concrete slab. A layered solid element was used to model the CFRP composites (Solid46). The element allows up to 250 different material layers with different orientations and orthotropic material properties in each layer. The element has three degrees of freedom at each node. Both longitudinal and transverse reinforcing bars are modeled using link element (LINK8).

Perfect bond between concrete and steel reinforcement bars was assumed since the bond between them is not a point of concern in this study. To provide this bond, the link element for the steel reinforcing was connected between nodes of each adjacent concrete solid element. The same approach was adopted for the connection between CFRP composites and the concrete surface of the slab. The high strength of the epoxy used to attach FRP sheets to the experimental beams supported the perfect bond assumption. A typical finite element mesh for a composite beam is shown in Fig. 16.

4.2 Material modeling

In compression, the stress-strain curve for concrete is linearly elastic up to about 30 percent of the maximum compressive strength; as shown in Fig. 17. Above this point, the stress increases gradually up to the maximum compressive strength. The steel reinforcement was assumed to be an elastic-perfectly plastic material; as shown in Fig. 18. Poisson's ratio of 0.3 was used for the steel reinforcement in this study Bangash (1989), Gere and Timoshenko (1997).

The unidirectional lamina has three mutually orthogonal planes of material properties (i.e., XY, XZ and YZ planes). The XYZ coordinate axes are referred to as the principal material coordinates where

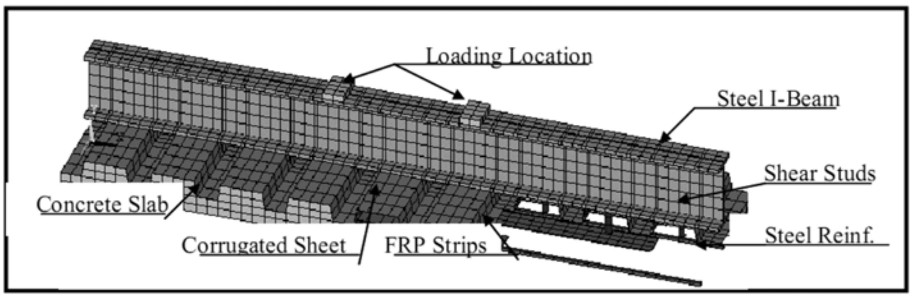

Fig. 16 Finite element mesh for models with corrugated sheet

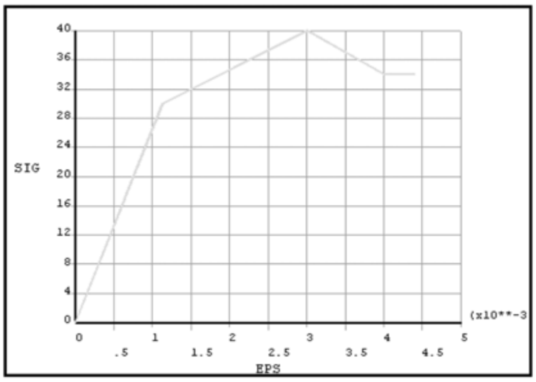

Fig. 17 Stress-strain curve for concrete

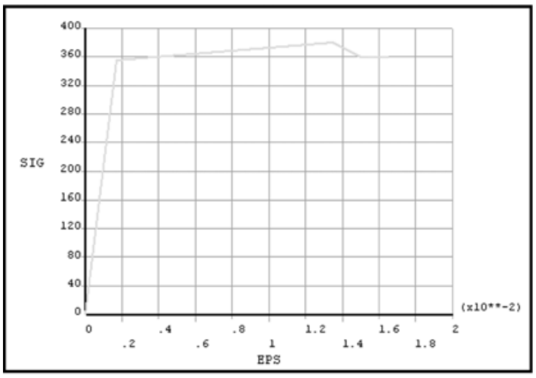

Fig. 18 Stress-strain curve for steel reinforcement

the X direction is the same as the fiber direction, and the Y and Z directions are perpendicular to the X direction. It is a so-called especially orthotropic material Gibson (1994), Kaw (1997). In this study, the especially orthotropic material is also transversely isotropic, where the properties of the FRP composites are nearly the same in any direction perpendicular to the fibers. Thus, the properties in the Y direction are the same as those in the Z direction.

4.3 Comparison with the experimental results

Comparison between the experimental and the finite element results presented to check the accuracy of the finite element simulation when CFRP strips are used. The general behavior of the finite element models represented by the load-deflection plots at mid-span shows good agreement with the test data; as shown in Fig. 19 and Fig. 20. However, the finite element models show higher stiffness than the test data in the nonlinear range, but the ultimate capacity of the strengthened beam using first principle was nearly the same strength from the finite element. The effects of bond slip; between the concrete and steel reinforcing; microcracks occurring in the actual beams were excluded in the finite element models and due to the full bond considered between the steel sheet and the concrete in the finite element model

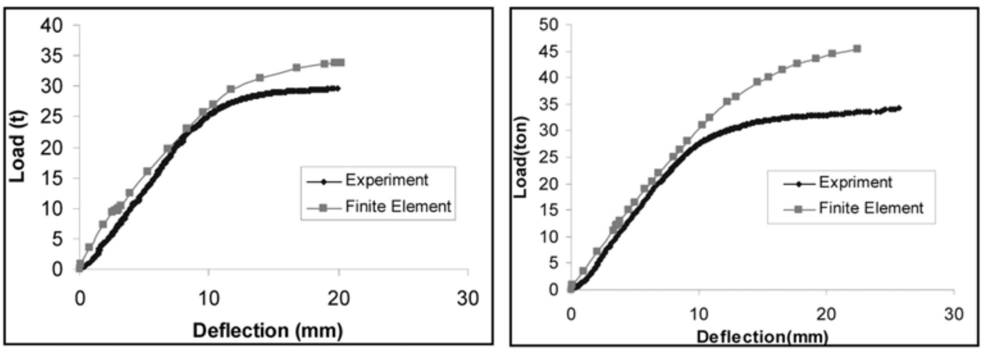

a) Reference beam (F1) b) Strengthened beam(F3)

Fig. 19 Load-deflection plot for beams of group one

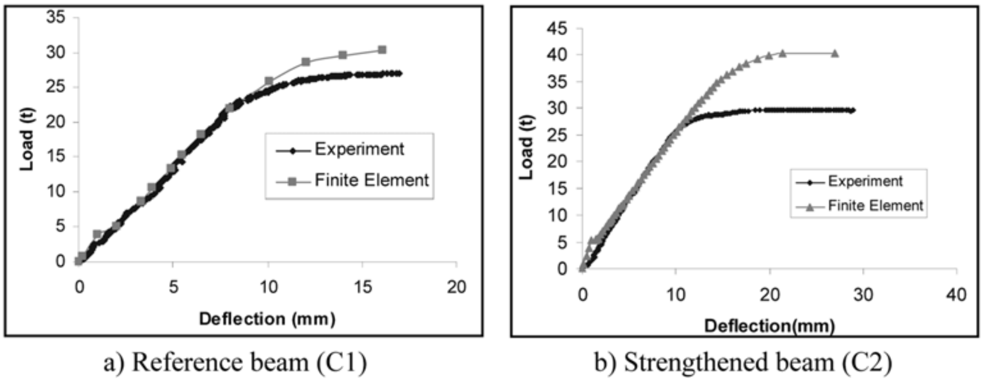

Fig. 20 Load-deflection plot for beams of group two

for beams of group two while in the experimental test 100% bond can not be reached perfectly, contributing to the higher stiffness of the finite element models.

5. Parametric study

It is difficult, expensive, and time consuming to optimize CFRP performance completely experimentally. Alternatively numerical models consider both concrete and CFRP properties through mechanical interaction provide a possible means of extending the available database. So, the effect of CFRP sheet arrangement, concrete strength and degree of shear connection on the behavior of the strengthened beams will be considered in the following section.

5.1 Effect of CFRP arrangement

Numerical analyses were carried out to investigate the effect of using the same width of CFRP sheets with different arrangements as 3-strips, 2-strips and 1-strip; as shown in Figs 21-23. The used

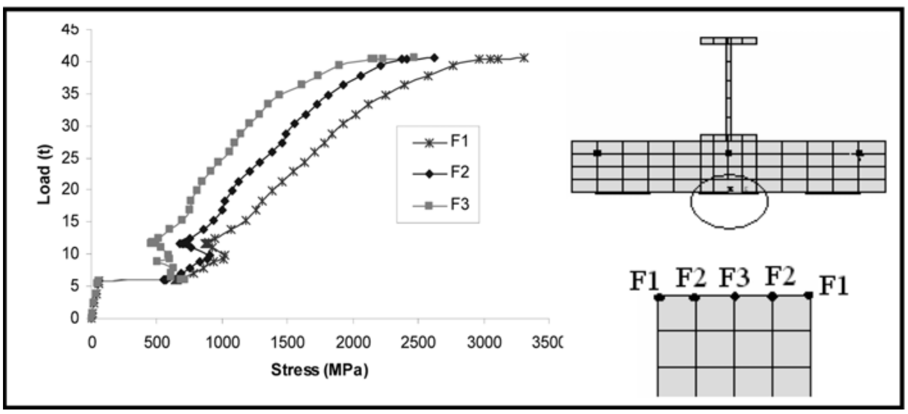

Fig. 21 Stress distributions across CFRP strip for 3-strips

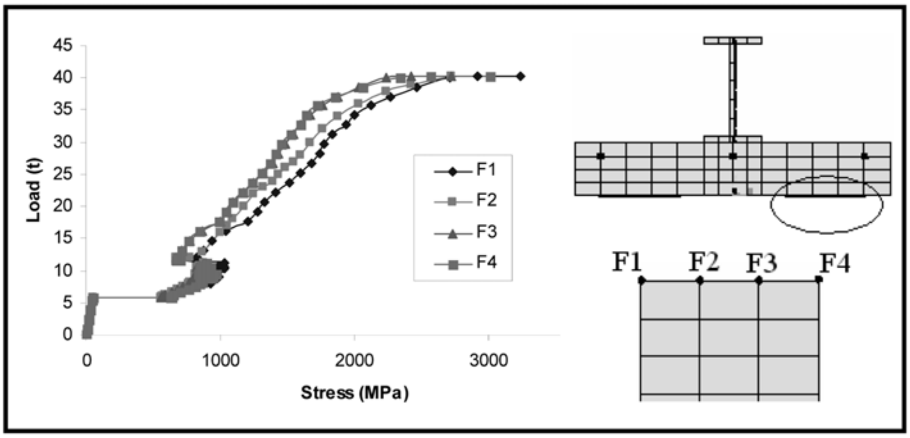

Fig. 22 Stress distributions across CFRP strip for 2-strips

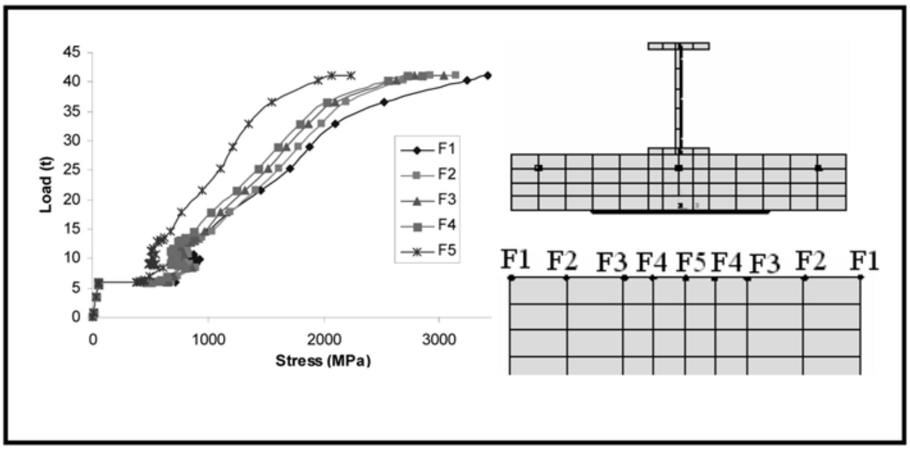

Fig. 23 Stress distributions across CFRP strip for -strip

numerical model did not have the debonding capability but was seen as sufficient to investigate the stress distribution across the CFRP sheet width. Figs. 21-23 show the stress distribution across the CFRP sheet width for 3-strips, 2-strips and 1-strip, respectively. It is noted that all points in the strip have the same stress until first cracks occur in the concrete slab and then drop in the stresses in the CFRP strip occurs. After the first cracks occur, the stresses at the edge of the strip were higher than the stresses in the center of the strip in the linear stage of the beam until the failure of the beam occur; the stresses become the same in all points a cross the strip. Due to the variation in the stress distribution across the CFRP sheet width as the width arrangement changes. The stresses at the edge of the CFRP sheets are higher than those at its center and the difference increases as the CFRP sheet width increases due to a shear lag effect in the concrete substrate. Fig. 24 shows comparison of maximum stress in CFRP strips for different arrangements. So, using 3-strips of CFRP sheets for this study is the best schemes for uniformly redistribution of stresses in the concrete slab. It also prevents any stress concentration and reduces the tension cracks along the width of the concrete flange.

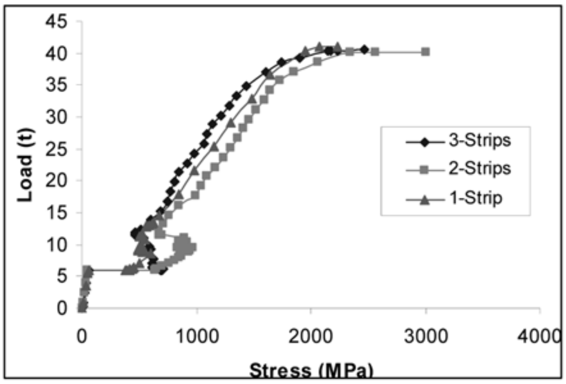

Fig. 24 Comparison of maximum stress in CFRP strips for different arrangements

5.2 Effect of concrete strength

The effect of concrete strength, f_{cu}, on the performance of CFRP sheets is studied using different values of concrete strength. The ultimate capacity is plotted against the concrete strength for all models with and without CFRP sheets; as shown in Fig. 25. The figures show that the increased capacity of the strengthened beam over the reference beam increases as the concrete strength increases. This indicates that the performance of CFRP sheets in the concrete slab increases as the concrete strength increases. Fig. 26 shows the stress in CFRP strips for different concrete strength. Stresses in CFRP strips increased as the concrete strength increased. Using CFRP sheets with high strength concrete will be more effective than that with low strength concrete.

5.3 Effect of shear connection

The following section presents the effect of the degree of shear connection between the slab and the steel I-beam on the performance of CFRP sheet used in strengthening concrete slab in composite beams. The degree of shear connection was modeled by changing the total number of the studs in the beam. The British Standards (BS 5950) and the Eurocode (EC 4) mentioned that the degree of shear

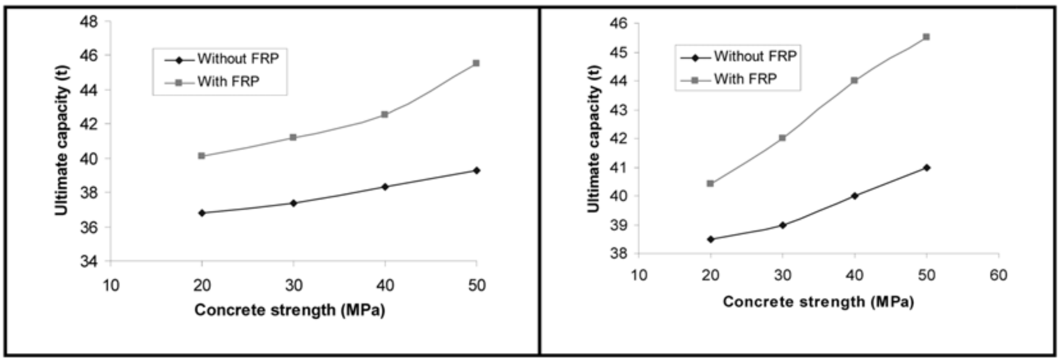

a) Composite beams without corrugated sheet b) Composite beams with corrugated sheet

Fig. 25 Ultimate capacity versus concrete strength

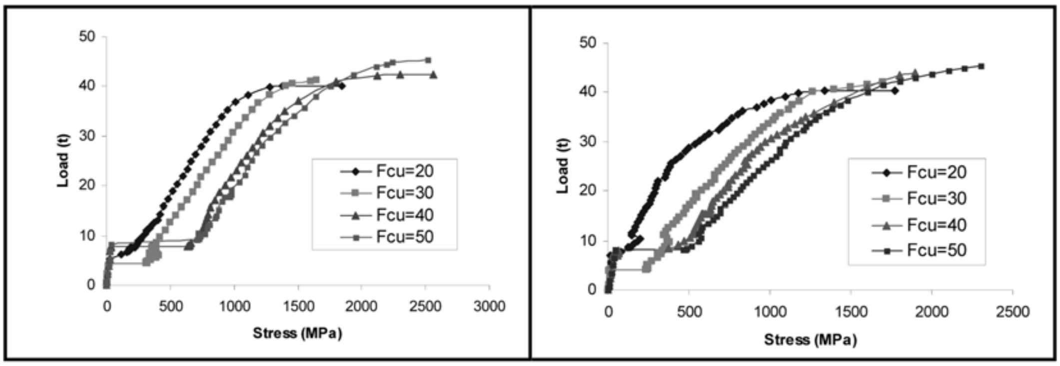

a) Composite beams without corrugated sheet b) Composite beams with corrugated sheet

Fig. 26 Max. stresses in CFRP strips

connection in composite beam subjected to hogging moment should not be less than 100%. However, some researchers, as Loh *et al*. (2004), had performed experimental and analytical studies on composite beams in hogging moment region with degree of shear connection starting from 33% up to 100%. They concluded that there was no significant reduction in the ultimate capacity of the beam due to decreasing in the shear connection. In this study, the effect of strengthening composite beams with CFRP sheets will be used in beams with degree of shear connection of 40% up to 100%.

Fig. 27 shows the ultimate capacity of the beam against the degree of shear connection for all models with and without CFRP sheets. It is noted that composite beams with and without CFRP sheets acted the same when the degree of shear connection was lower than 60%. This was because the failure was due to the shear connection. Increasing the connection made it possible to the CFRP sheet to enhance the behavior of the composite beam and increase its capacity.

The effect of using CFRP sheet for strengthening slab in composite beams subjected to negative moment increased as the degree of shear connection increased. To obtain the full benefit of using CFRP sheet in strengthening the concrete slab, the degree of shear connection for composite beams should be increased to 80% shear connection or higher.

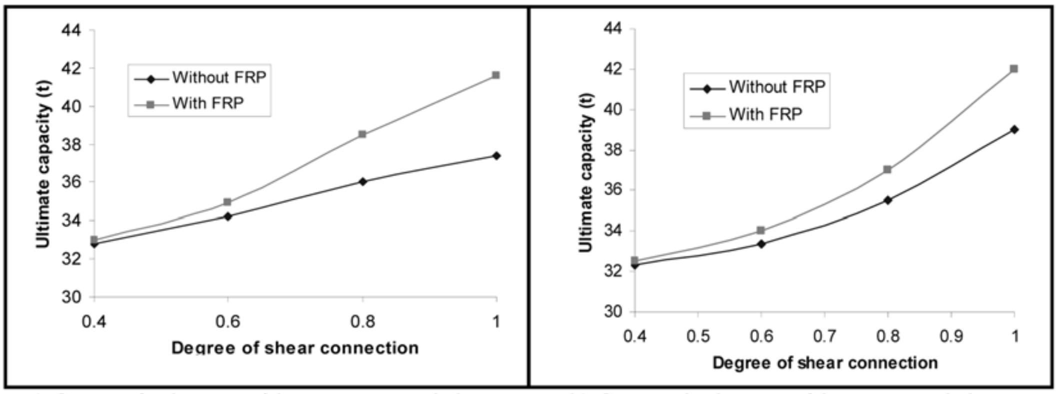

a) Composite beams without corrugated sheet b) Composite beams with corrugated sheet

Fig. 27 Degree of shear connection against ultimate capacity

6. Conclusions

Strengthening composite beams with concrete slab with CFRP sheets increased the load carrying capacity of the beam by 15%. This increase is related to the thickness of the CFRP sheet; doubling the sheet thickness increased the ultimate capacity of the beam up to 21%.

The load carrying capacity of the flexure strengthened beams with corrugated sheet predicted by the experimental data is higher than that of the control beam by 12%. No failure was noticed in the CFRP strips and no tensile cracks in the upper surface of the concrete slab as well. The CFRP strips prevented the concrete slab failure as happened in the unstiffened beam. This indicates the importance of increasing the bond between the concrete and the profile steel sheet in negative moment regions to get the full benefit of the effect of CFRP sheets in this region.

Using the same width of CFRP sheets is more effective as strips than one strip where the stress at the edge of the CFRP sheets are higher than those at its center and the difference increases as the CFRP sheet width increases due to a shear lag effect in the concrete substrate.

The stress at the edge of the CFRP sheets are higher than those at its center and the difference increases as the CFRP sheet width increases due to a shear lag effect in the concrete substrate. So, good attachment especially at the edges of the CFRP sheets is recommended to avoid peeling of the sheets.

Using CFRP sheets in composite beams with high strength concrete will be more effective than that with low strength where the performance of CFRP sheets took effect and enhanced the whole behavior of the beam.

80% degree of shear connection or higher is recommended for composite beams subjected to negative bending moment to achieve good behavior of the beam and to obtain the desired performance of the CFRP sheets in strengthening composite beams under this type of straining actions.

References

ANSYS Element Manual, Tenth Edition, Swanson Analysis System Inc.

Ashour, A.F., El-Refaie, S.A. and Garrity, S.W. (2004), "Flexural strengthening of RC continuous beams using CFRP laminates", *J. Cement. Concrete. Compos.*, 26, 765-775.

Bangash, M.Y.H. (1989), *Numerical modeling and applications*, Elsevier Science Publishers Ltd., London, England.

British Standard Institution (1990), Structural use of steel work in building, Part 3, Section 3.1: Code of practice for design of composite beams, BS 5950, BSI, London.

Buyukozturk, O., Gunes, O. and Karca, E. (2004), "Progress on understanding debonding problems in reinforced concrete and steel members strengthened using FRP composites", *Constr. Build. Mat*., **18**(1), 9-19.

Donnet, J-P. and R.C. Bansal. (1990), *Carbon fibers*, Marcel Deckker, Inc., New York.

Eurocode 4 (1992), Design of composite steel and concrete structures, Part 1.1: General rules and rules for buildings, Commission of the European communities.

Gao, B., Leung, C.K.Y. and Kim, J.K. (2005), "Failure diagrams of FRP strengthened RC beams", *J. Compos. Struct.*, 1-16.

Gere, J.M. and Timoshenko, S.P. (1997), *Mechanics of materials*, PWS Publishing Company, Boston, Massachusetts.

Gibson, R.F. (1994), *Principles of composite material mechanics*, McGraw-Hill, Inc., New York.

Kaw, A.K. (1997), *Mechanics of composite materials*, CRC Press LLC, Boca Raton, Florida.

Li, L.J., Guo, Y.C., Liu, F. and Bungey, J.H. (2006), "An experimental and numerical study of the effect of thickness and length of CFRP on performance of repaired reinforced concrete beams", *J. Constr. Build. Mat.*, **20**(10), 901-909.

Loh, H.Y., Uy, B. and Bradford, M.A. (2004), "The effect of partial shear connection in the hogging moment regions of composite beams. Part I-Experimental study", *J. Constr. Steel. Res.*, **60**(6), 897-919.
Loh, H.Y., Uy, B. and Bradford, M.A. (2004), "The effect of partial shear connection in the hogging moment regions of composite beams. Part II-Analytical study", *J. Constr. Steel. Res.*, **60**(6), 921-962.
Mertz, D.R. and Gillespie, J.W. (1996), "Rehabilitation of steel bridge girders through the application of advanced composites materials", Final Report, NCHRP-93-ID011, TRB. Washington, DC: National Research Council.
Sen, R., Liby, L., Spillet, K. and Mullins, G. (1995), "Strengthening steel composite bridge members using CFRP laminates", *Proceedings of the second international RILEM symposium on non-metallic (FRP) reinforcement for concrete structures*, Ghent, Belgium.
Sikadur-330 (2005), "Impregnation resin for fabric reinforcement", Version no. 01.03.
Sikawrap Hex-230C, "Carbon fiber fabric strengthening system", Version no. 05.04.
Teng, J.G. and Smith, S.T. (2002), "FRP-strengthened RC beams. II: assessment of debonding strength models", *J. Eng. Struct.*, 24, 397-417.
Wipf, T.J., Saidy, A.H. and Klaiber, F. W. (2007), "Strengthening of steel concrete composite girders using carbon fiber reinforced polymer plates", *Constr. Build. Mat.*, **21**(2), 295-302.

CC